Selected aspects of geometrical analyses of surfaces measured using terrestrial laser scanning (TLS)

Janina Zaczek-Peplinska, Maria Elżbieta Kowalska, Krystian Ryczko, Cezary Sekular

Faculty of Geodesy and Cartography, Warsaw University of Technology, Politechniki Square 1, 00-661 Warsaw, Poland, (janina.peplinska@pw.edu.pl; maria.kowalska@pw.edu.pl; krystian.ryczko.stud@pw.edu.pl; cezary.sekular.stud@pw.edu.pl)

ABSTRACT

Modern measurement technologies are widely used for the monitoring and determination of surface deformations. One more frequently used measurement technology is terrestrial laser scanning (TLS), which provides quasi-continuous information about the tested surface in the form of a point cloud at a given resolution. At the same time, TLS is based on measuring the distance in a given direction, thanks to which we can obtain a high precision of measurement, often compared to tacheometric measurements. This paper presents a study on the determination of surface flatness parameters extracted from a point cloud. It takes into account the roughness characteristics of the different structures on the measured surfaces and analyzes them using the most popular algorithms for determining the distance of points from the reference surface. Additionally, the review presents the issue of expanding selected surfaces onto a plane to analyze their geometric parameters, and thus to determine the deformation. The applied solution can be used to monitor the deformation of objects such as tunnels and interiors of collectors or large-diameter downpipes, the shape of which is similar to a cylinder surface. Thanks to the expansion of the cylinder surface into a plane, it is possible to perform a comprehensive analysis of surface deformation, and not only selected fragments in the form of sections. The conducted analyses show the great potential of data obtained using terrestrial laser scanning, when an appropriate procedure and data processing method are applied. This paper focuses on two types of studies; the study of surface flatness and analysis of the deformation of cylindrical surfaces. These types of studies are extremely useful in assessing the technical condition of structures, especially in studying the deformation of structures built underground (tunnels, passages, warehouses), where the loads from the surrounding earth are significant.

I. INTRODUCTION

A. *Terrestrial Laser Scanning*

The main purpose of the research presented in the paper is to indicate the possible use of the terrestrial laser scanning in assessing the condition of structures, especially deformations in underground structures (tunnels, passages, warehouses) with significant loads from the surrounding ground. This article presents generally available tools thanks to which it will be possible to widely use the proposed solutions in commercial analyses of deformations in engineering objects. Terrestrial laser scanning (TLS) technology is widely used for the monitoring and determination of surface deformations (Harmening *et al.*, 2021; Yang *et al.*, 2021; Gawronek *et al.*, 2019; Kovanič *et al.*, 2019; Liu *et al.*, 2020). It provides quasi-continuous information about the surveyed surface in the form of a point cloud with *X,Y,Z* coordinates, complemented by the reflection intensity. Terrestrial laser scanning is based on the measurement of distance in a specified direction and gives high precision measurements comparable to tacheometric measurements. It makes it

possible to monitor a greater number of points on surfaces and from practically any place, provided that an appropriate point cloud resolution is maintained. For the assessment of deformations of the surface of a structure, the scanning resolution is selected based on the geometry of the surveyed structure, the measurement plan and the expected deviations from the norm.

B. *TLS data quality*

Terrestrial laser scanning, like any other measurement technology, is subject to a variety of measurement errors. Many publications have detailed the significance of appropriate calibration of terrestrial laser scanners (Medić *et al.*, 2020; Reshetyuk, 2006; Abbas *et al.*, 2013; Li *et al.*, 2018), while equipment manufacturers use increasingly advanced technical solutions and algorithms to improve the accuracy of the acquired data. While the problem of external errors still remains, they have an influence that is difficult to model and which greatly affect the accuracy of the geometric data and recorded spectral values. Knowledge of the factors that affect the quality of TLS

data, such as systematic and random errors, is crucial in performing reliable analyses. Wang *et al.* (2016) introduced some mathematical modeling of external errors and how it can be applied in real TLS measurements. Their results revealed an up to 50% increase in point cloud accuracy; however, the authors emphasize that this remains difficult and is still an unsolved issue. Errors affecting the quality of TLS data can be divided by their various factors. For example, Kashani *et al.* (2015) divided them into four main categories: (i) target surface characteristics (reflectivity and roughness), (ii) data acquisition geometry (range and incidence angle), (iii) instrumentation effects, and (iv) environmental influences.

The occurrence of the various types of errors in measurements has a direct impact on the quality of the analyses performed with the point clouds and requires an appropriate methodology. This paper focuses on two types of studies: the study of surface flatness and analysis of the deformation of cylindrical surfaces. These types of studies are extremely useful in assessing the technical condition of structures, especially in studying the deformation of structures built underground (tunnels, passages, warehouses), where the loads from the surrounding earth are significant.
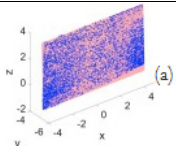
II. MATERIALS AND METHODS

A. *Surface flatness test*

The first issue addressed in this paper is the study of surface flatness. This task is performed in the context of many engineering structures, a classic example being large floor areas of facilities or high storage warehouses, which must meet increasingly demanding flatness criteria. The situation is analogous to the context of road surfaces, squares and other engineering structures which are subject to inspections checking their compliance with design requirements or standards (Wyczałek *et al.*, 2017). Therefore, it is safe to say that the quality control of flatness is essential in construction. There is a growing need to propose an automated and rapid approach for flatness quality assessment to replace the tedious traditional manual measurement methods (Li *et al.*, 2020), hence the increasing use of terrestrial laser scanning for this task, allowing the registration of millions of survey points in a very short time. The study of surface flatness based on a point cloud can be implemented in two ways. In the first variant, the plane is fitted to the measured points, *e.g.* by the method of least squares. This solution is connected with the problem of selection of measured points that actually represent the flat surface and are not measurement noise or were not measured in the places of surface deformation. The second variant is testing flatness of the surface by comparing it with a theoretical model, but in this case it is necessary to provide a common orientation for the measured surface and its model.

Reliably fitting a plane to a point cloud requires an assessment of the accuracy of the fit. Table 1 summarizes the equations used to fit the plane (Ye *et al.*, 2018).

Table 1. Parameters for fitting a plane to a point cloud (Ye *et al.*, 2018)

	Plane fit
Diagram	
Equation (vector form)	(**p**-**p₀**)*n=0, where **n**=(nx,ny,nz) is the normal vector of the plane, **p₀**=(x₀,y₀,z₀) is a point on the plane, and **p**=(x,y,z) is a point in the point cloud
Equation (Cartesian form)	Ax+By+Cz+D=0

Evaluation of the accuracy and quality of the fit can be made based on the global plane fitting error - e_a (Eq. 1) (Qian and Ye, 2014). For an extracted plane containing M data points, the plane-fitting error is given by:

$$e_a = \sqrt{\frac{\sum_{i=1}^{M} d_i^2}{M}} \qquad (1)$$

where d_i = the distance from the ith data point to the plane

One publication (Ye *et al.*, 2018) also proposes evaluating the accuracy of the plane fit based on the formula for the distance of a point from the plane (Eq. 2).

$$e = \frac{Ax_i + By_i + Cz_i + D}{\sqrt{A^2 + B^2 + C^2}} \qquad (2)$$

where e = point position error
A, B, C, D = parameters of the plane equation in Cartesian notation
$x_i, y_i, z_i,$ = point in the point cloud

It should be noted that when fitting a plane to a point cloud using the least squares method, we minimize the distances of the points from the surface, and thus the question arises whether such a fitted plane is an appropriate basis for evaluating the surface flatness. A solution to this dilemma could be to select points (randomly or a certain percentage) to represent the surface and use these to fit a reference plane (Ye *et al.*, 2018). However, this raises another question of which criteria should be used to select these points. A solution may be in selection of the areas of the surface for which, with a high probability based on analysis of the design and the results of archival measurements (if

performed), there are no deformations, *e.g.* in the vicinity of contact with other surfaces, in places where the structure is stiffened by additional supports, etc.

A second very important aspect in the context of analysis of surface flatness is surface roughness, which will affect both the accuracy of fitting the plane to the cloud and the determination of local deformations.

The classification of surface roughness according to Eurocode 2 distinguishes three types of surface: very smooth, smooth and rough. This classification is distinctly inexact as it depends on the subjective estimation of the designer. Selection of the most relevant 3D roughness parameters is a key issue (Muszyński and Wyjadłowski, 2020). The most popular parameters that determine the surface roughness, written in a mathematical way, are summarized in Table 2.

Table 2. Selected surface roughness parameters (Eurocode 2)

Parameter	Equation
Root-mean-square height	$S_q = \sqrt{\dfrac{1}{A} \iint_A (Z(x,y))^2 dxdy}$
Maximum peak height	$S_p = sup\{Z(x_i, y_i)\}$
Maximum pit height	$S_v = |inf\{Z(x_i, y_i)\}|$
Maximum height	$S_z = S_p + S_v$

It is worth noting that these parameters are determined with respect to a line or mean surface, which again leaves room for discussion in the context of fitting a plane to a point cloud and their use in the context of determining the parameters of that plane. In the next part of the article we will try to deal with these problems.

Surface flatness testing is also applied in quality inspection and acceptance of a tunnel project (Xiang *et al.*, 2021), hence the second issue considered in this paper is the development of selected cylindrical surfaces into a plane.

B. *Expansion of selected surfaces to a plane*

The expansion of selected surfaces into a plane is an effective method of presenting measurement results of complex objects by terrestrial laser scanner. Currently, the process of identifying individual technical elements and defining the spatial structure of the object takes place in the three-dimensional space of the point cloud, and the final elaborations are made in the form of local cross-sections. This approach makes the data analysis more difficult and reduces the potential use. In the case of large and complex structures, analyses require selecting a particular fragment of the point cloud and performing local analyses. Otherwise, the displayed point cloud is unreadable due to overlapping points in the current perspective or in the orthogonal view. The solution to this problem is to use surface expansion to a plane. This approach is used both for objects with known geometry such as a sphere or cylinder (Xu *et al.*, 2019; Pinpin *et al.*, 2021) and for more complex objects such as telecommunication antennas (Dabrowski *et al.*, 2019). Dabrowski and Specht (2019) present the advantages of using spatial expansions:

1. Improved legibility of the measured point cloud of the object.
2. Obtaining information about the distance of the point from the object construction axis in the form of the coordinate of the projected point cloud.
3. Obtaining information about angular spatial configuration of individual elements of a measured symmetrical object.
4. Ability to create two-dimensional datasheets containing detailed geometric and descriptive information on the point cloud.

In that paper, the authors focused on the development of a cylinder surface as a shape that is representative for tunnel objects. The spatial projection of a point cloud onto the side surface of a cylinder requires the determination of three parameters. Two of them are linear parameters and the third is an angular parameter. The first is the radius of the cylinder - *R*. Evaluation of the parameter depends on the spatial structure of the point cloud and has a direct influence on the distortion distribution in the expansion. Performing the projection is possible for any non-zero value of the parameter *R*. However, the optimal choice of the cylinder radius determines the distortion distribution and directly affects the readability of the final product (Dabrowski and Specht, 2019). The second, a linear parameter, is the horizontal distance from the vertical extension axis *h*. While the angular projection parameter is ϕ, the direction of point *P* is relative to the initial direction of expansion in the horizontal XY plane (Dabrowski and Specht, 2019).

The functions of the spatial projection of a point cloud to the lateral of the cylinder in matrix notation (Eq. 3) are expressed in the following formulas:

$$\begin{bmatrix} x_P^R \\ y_P^R \\ z_P^R \end{bmatrix} = \begin{bmatrix} U(x_P, y_P) \\ V(z_P) \\ W(x_P, y_P) \end{bmatrix} = \begin{bmatrix} R * \Phi(x_P, y_P) \\ z_P \\ h(x_P, y_P) \end{bmatrix} \quad (3)$$

where x_P^R, y_P^R, z_P^R = projected (spatially expanded) point coordinates
$U(x_P, y_P)$, $V(z_P)$, $W(x_P, y_P)$ = spatial projection functions
x_P, y_P, z_P = coordinates of the point of the original surface (point cloud)
R = cylinder radius
$\phi(x_P, y_P)$ = direction angle of point P (angular parameter of the expansion)
$h(x_P, y_P)$ = point distance from the expansion axis (linear parameter of the expansion)

Developing a point cloud representing a cylindrical surface into a plane allows for many analyses and a simplified representation of the surface deformation. In the case of a deformation, we can use methods analogous to surface flatness analysis.

C. *Research Facility - Subway Tunnel*

In this paper, the flat ceiling of the entrance hall and a fragment of the connecting tunnel built to connect the 1st line with the 2nd line of the Warsaw Metro were used as the test object. The analyzed tunnel runs along a curve between the hall with side tracks on the east side of the C-10 Rondo ONZ station on Line II and the hall with side tracks on the north side of the A-13 Centrum station on Line I. It has a technical function, so it does not serve regular passenger traffic. A tunnel boring machine was used to create it, and as a result it is encased in distinctive rings made of concrete. There is a concrete platform in the tunnel along the track.

III. RESULTS

A. *Development of terrestrial laser scanning data*

For the study, measurements were taken with a Leica RTC360 laser scanner, which has a scanning speed of up to 2 million points/sec, a declared scanning resolution of 3 mm, 6 mm or 12 mm at 10 m, an angular accuracy of 18", a distance measurement accuracy of 1 mm + 10 ppm, and a 3D point position accuracy of 1.9 mm (at 10 m) and 2.9 mm (at 20 m). The measurements included two components: the ceiling of the entrance hall and the connecting tunnel itself. The point cloud orientation process was performed using Leica Cyclone Register360 software. The mutual orientation of the acquired point clouds was performed on the basis of automatic detection of the object's features, while the external orientation of the entire object to the PL-2000 state space reference system was performed on the basis of known target coordinates. The accuracy of the performed point cloud orientation process is determined by the parameters: Bundle Error, Overlap, Strength, Cloud-to-Cloud and Target Error (Table 3). Each scan orientation has its own accuracy characteristics, and bundle error is a parameter that determines the accuracy of the entire combination of scans. The overlap parameter defines the percentage of overlap between each configuration. The strength parameter defines the relative stiffness of all bindings in arbitrary directions. The last parameter is cloud-to-cloud, whose value indicates the mutual fit of the point cloud geometries, thus preserving the characteristics of the measured object. The obtained point cloud orientation parameters were found to be satisfactory.

B. *Surface flatness*

As already mentioned, performing a scan of horizontal elements is one of the basic issues of engineering geodesy. The effects of such measurements are most often compared with the design and then communicated to the responsible persons, *e.g.* construction management. However, we do not always have a three-dimensional base model of the object which can serve as a reference surface for the flatness analysis. This paper presents examples of surface flatness analysis based on comparing a point cloud to a surface fitted using the least squares method. Figure 1 presents the analyzed point cloud in intensity colors recorded for the entrance hall of the connecting tunnel.

Table 3. Accuracy parameters of the conducted orientation

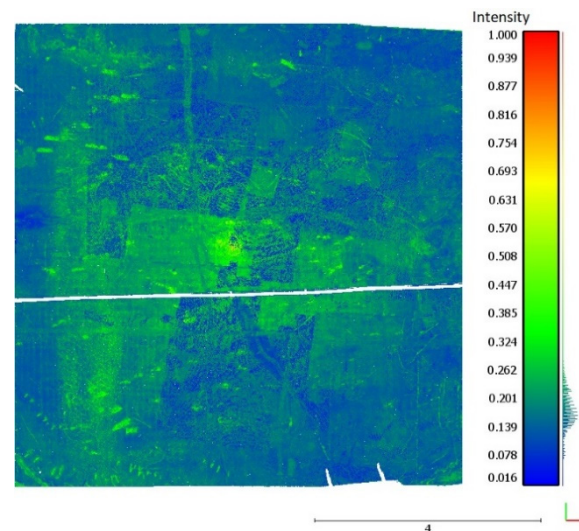| Parameter	Connecting tunnel
Bundle error [mm]	0.001
Overlap	60%
Strength	54%
Cloud-to-Cloud [mm]	0.001

Figure 1. Point cloud representing the ceiling of the entrance hall of the connecting tunnel in intensity colors.

Based on the acquired data, the analysis was performed in two variants. The first variant involved fitting a plane to all the measured points and then determining the distance of the points from the plane using the Cloud To Mesh (C2M) algorithm (Figure 2).

For the analysis performed, the value of the global plane fitting error was determined to be e_a=6.4 mm. In the second variant, only some points were used to fit the plane. For this purpose, a frame was cut out of the basic point cloud (Figure 3) and then the plane was fitted into it. This approach was based on the assumption that the ceiling plane undergoes the least deformation at the point of contact with vertical walls (which resulted from the design).

Figure 4 presents a map of the distances of points from the plane defined in variant II, determined by the Cloud To Mesh (C2M) algorithm. The global plane fitting error value was e_a= 8.7 mm.
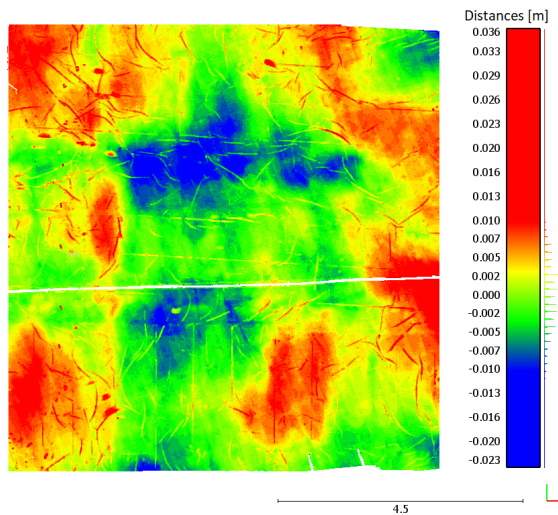
Figure 2. Cloud To Mesh (C2M) distance analysis for a section of the entrance hall ceiling using a reference plane fitted to all measured points.
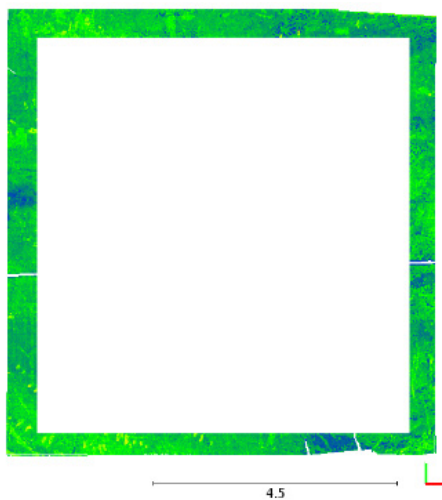

Figure 3. A set of points located at the floor-wall interface selected as the reference frame for the surface fit.
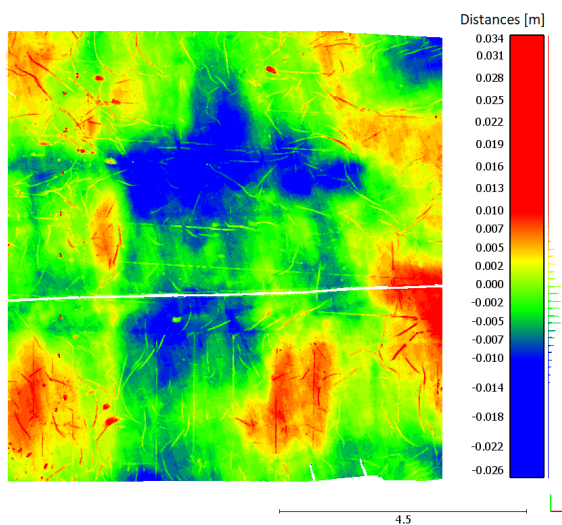

Figure 4. Cloud To Mesh (C2M) distance analysis for a section of the entrance hall ceiling using a reference plane fitted to a selected frame (Figure 3).

The comparison of distance maps determined by the C2M method for reference planes determined in two different ways (Figure 2 and 4), as well as the analysis of histograms of C2M distances (Figure 5 and 6) for these two variants, indicate the great importance of the selection of points as the basis for determining the plane parameters. The choice of the plane directly affects the results of the comparisons, and thus the analyzed values of deviation from the flatness of the surface. In both analyzed cases, the trend of changes looks similar. Figures 2 and 4 both show two significant areas in blue where the ceiling is curved towards the floor, yet the values obtained in both cases differ. In the case of the area shown in Figure 2 most of the points are between -0.01 m and 0.01 m, while in the case of the area shown in Figure 4, the distances of the points from the reference plane are mostly between -0.02 m and 0.01 m. Figures 5 and 6 show histograms of the distribution of point distances from the plane for both variants of the plane definition.
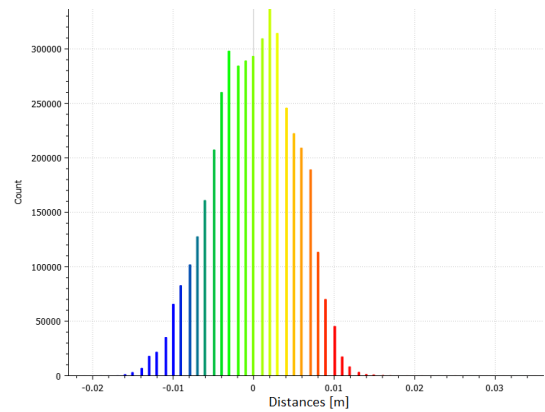

Figure 5. Cloud To Mesh (C2M) distance histogram for a section of the ceiling of the entrance hall of the connecting tunnel, using a reference plane fitted to all measured points.
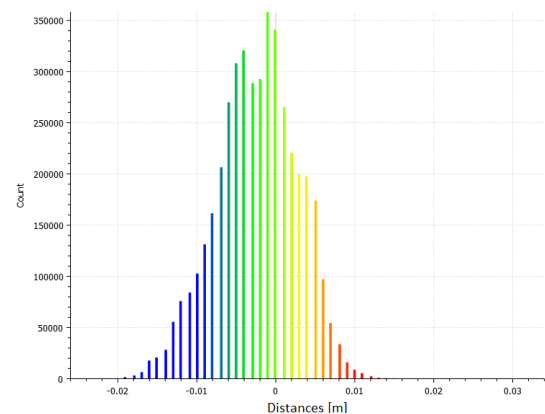

Figure 6. Cloud To Mesh (C2M) distance histogram for a section of the ceiling of the entrance hall of the connecting tunnel, using a reference plane fitted into a selected frame (Figure 3).

Table 4 lists the values of the normal vectors for the fitted planes in both variants. As can be seen, the differences are small (on the order of 1/10,000), and the values of the normal components in the Z direction indicating the horizontality of the plane are the same.

393

Table 4. Normal vectors of the designated planes

	Normal vector of the plane
Plane fitted to the entire point cloud	(0.00369531; 0.00127337; 0.999992)
Plane fitted to a sample frame	(0.00388479; 0.000977652; 0.999992)

Table 5 summarizes the roughness parameters determined based on the plane fitted to all points and the plane fitted to the points forming the frame in Figure 3. Based on the summarized quantities, it can be concluded that even a slight difference in the definition of the reference plane affects the determined roughness parameters.

Table 5. Roughness parameters determined based on the plane fitted to all points and the plane fitted to the points forming the frame in Figure 5

Parameter	Fitting a plane into the whole cloud [m]	Fitting a cloud into a frame [m]
Sq	0.006	0.009
Sp	0.035	0.033
Sv	0.023	0.026
Sz	0.058	0.059

In Figure 7, the authors have presented a histogram of the distribution of the Z coordinate for the investigated floor surface. The dominant value is $Z = 78.000$m, which indicates that it is possible to undertake a deformation analysis of the floor with respect to a horizontal plane located at a constant height of 77.995 m.
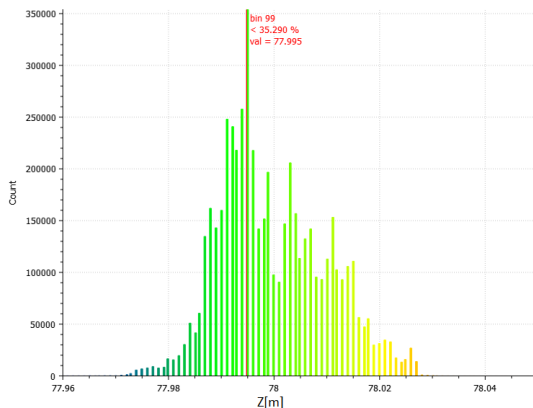

Figure 7. Histogram of the Z-coordinate distribution for the tested floor area.

The differences in the distances of the points from the horizontally defined plane at 77.995 m are shown in Figure 8. The distance distribution obtained clearly indicates the slope of the floor on the left side.

The analyses of distances of points from variously defined planes show the importance of proper selection of the definition of the reference surface.

C. Expansion of the tunnel surface into a plane

The next stage of analysis is the cylindrical fit based on the acquired point cloud. For this purpose, the function implemented in CloudCompare software was used, built on the basis of the Automatic RANSAC Shape Detection method with Schnabel's modifications (Schnabel *et al.*, 2007). The tool is composed of 5 basic parameters: the minimum number of points defining a given shape, the parameter e - the maximum distance of a point to the analyzed model, the parameter b - the resolution of the point cloud, the parameter a - the maximum deviation of the best fitted cylinder shape with respect to the normal vector (expressed in degrees), and the probability parameter (Marjasiewicz and Malej, 2014). For the above-mentioned parameters, there is no single correct value. In the case of the presented problem, the authors performed a number of tests to select the most optimal parameter values. The basic assumption of the performed tests was to obtain the best-fitting cylinder model. The criteria for the selection of the best solution was to obtain the nominal value of the radius of the tunnel casing - 2.7 m, and to select the largest number of points for the fitting process. Empirically determined parameters take the following values: minimum number of points - 500 000, $e = 2$ cm, $b = 4$ cm, $a = 25°$, overlook probability = 3 cm.
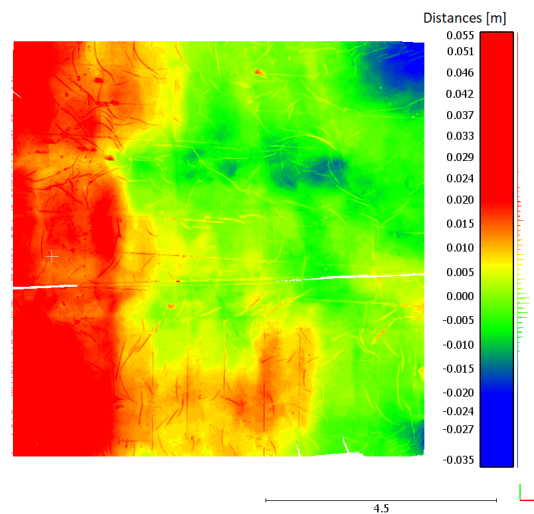

Figure 8. Analysis of the distance of points from the ordinate of 77.995 m for the section of the ceiling of the entrance hall of the connecting tunnel.

Figure 9 presents the relation of the initial point cloud to the cylinder model expressed by the distance of points from the model surface (algorithm - C2M).

The values presented in the color scale in Figure 9 range from -5 cm (blue color) to +5 cm (red color). The dominant colors for the first part of the tunnel are shades of green and shades of yellow - in the range - 2 cm to +3 cm. For the second fragment of the object, undulations and high color contrast resulting from the geometry of the object are visible. This results in larger differences contained in the whole span of the selected

range. Hence empty fields can be observed, which result from the fact that in these parts the distances are longer than 5 cm in absolute values. Additionally, 5 cm wide "stripes" are noticeable, representing all elements of the technical equipment of the subway tunnel, *i.e.* tracks, platforms.
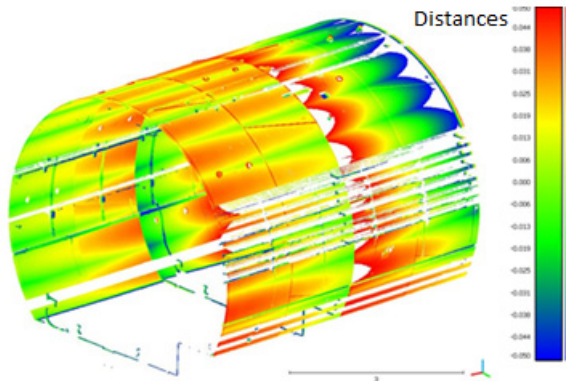

Figure 9. Relation of the initial point cloud to the cylinder model (C2M).

In the next step, the point cloud representing the tunnel fragment was expanded onto a plane. For this purpose, the unroll function in CloudCompare software was used. Its parameters included:

- Expansion type.
- The parameter that defines the figure - in the case of a cylinder, it is the radius.
- Axis - select the axis around which the expansion is performed.
- Base point - which determines the position of the selected axis in space.
- The angle of expansion - determining what part of the cylinder is subject to expansion.

The results of the expansion are presented in Figure 10, on the left is the expanded point cloud in intensity colors, while on the right is the analysis of the distance of the points (C2M algorithm) from the fitted plane using the least squares method.
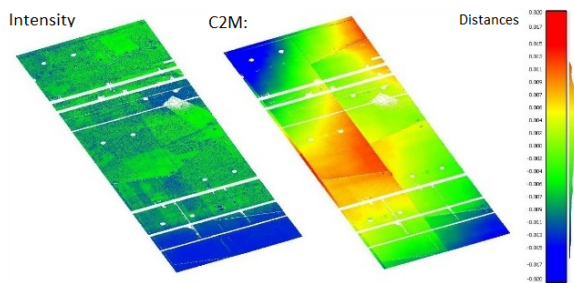

Figure 10. Expansion results, on the left the expanded point cloud in intensity colors, on the right the analysis of the distance of the points (C2M algorithm) from the fitted plane based on the least squares method.

The parameters adopted for the development include the nominal radius value, the angle of development of the whole - from 0 to 360 degrees, and the base point defined as the center of gravity of the cylinder. A color

scale was adopted for the roll-out, with distances ranging from -20 mm to +20 mm. The central part of the roll-out is dominated by green, yellow and orange colors, with values ranging from -4 mm to +10 mm. The upper left and lower right ends are dominated by blue, which corresponds to the largest differences - a value of about -15 mm. The situation is different between the opposite ends, with the upper right corner having a value of about +10mm and the lower left corner having an extreme of -7 mm. The mentioned values are influenced by taking into account a section consisting of 2 tubing units, which causes some curvature. However, this approach has highlighted the joints between the individual precast elements. It should be noted that some of the precast elements differ significantly in color, which leads to the conclusion that there are shifts - deformations between them. In the middle part of the expansion, at the border of two tubing units, there is a sudden peak of color, where it can be concluded that the difference between the position of these precast elements is about 7 mm. There are white circles on the expansion – being remnants after removing the prefabricate fixings in the process of manual filtering of the point cloud.

IV. Discussion

This paper presents both a theoretical basis and the results of practical analyses related to fitting a plane to a point cloud. Analyses of the distances of the points from the variously defined planes show the importance of a proper choice of a reference surface definition. Fitting the plane to all the measured points, according to the definition of the method of least squares, will minimize the distances of the points from the plane, and thus show the trend of changes, but not their actual values. The second variant presented in this paper, in which the plane is fitted to points forming the contact frame with supports (in this case the walls), a fixed base for fitting, allows the plane to be defined by excluding the points representing the actual deformation of the surface. Hence the slight differences in the results obtained with respect to the first variant. Also in this case we do not have the certainty of whether the points forming the frame were not registered in the area where the surface change occurred. Therefore the authors undertook another analysis in which they assumed that the reference surface is ideally horizontal and the choice of its height was based on the histogram of the *Z* coordinate for the examined ceiling surface. In this case the analysis indicated a clear slope of the ceiling towards the right side.

The second aspect presented in this paper concerned analysis of the surface deformation mapped with cylindrical unfolding of a subway tunnel in Warsaw. In this case, the authors proposed to perform an expansion of the scanned surface into a plane so that it will be easier to represent the changes, and it will be

2022, Editorial Universitat Politècnica de València

possible to apply the conclusions drawn from the analysis of the plane.

The methods of flatness analysis and deformation assessment proposed in this article are applicable to many tasks in the field of engineering geodesy performed at a construction site, with their results and interpretation having a real impact on the safety measures and construction works. In our opinion, increasing the reliability of analysis results is very important to ensure the structure's safety.

References

Abbas, M. A., H. Setan, Z. Majid, A.K. Chong, K.M. Idris, and A. Aspuri (2013). Calibration and accuracy assessment of leica scanstation c10 terrestrial laser scanner. In: *Developments in Multidimensional Spatial Data Models*. Springer, Berlin, Heidelberg, pp. 33-47.

Dabrowski, P. S., and C. Specht (2019). Spatial expansion of the symmetrical objects point clouds to the lateral surface of the cylinder-Mathematical model. *Measurement*, Vol 134, pp. 40-47.

EN 1992-1-1:2004 Eurocode 2: Design of concrete structures - Part 1-1: General rules and rules for buildings, (2004).

Gawronek, P., and M. Makuch (2019). Tls measurement during static load testing of a railway bridge. *ISPRS International Journal of Geo-Information*, Vol. 8(1), pp. 44.

Harmening, C., Hobmaier, C., and Neuner, H (2021) Laser Scanner–Based Deformation Analysis Using Approximating B-Spline Surfaces. *Remote Sens.*, *13*, 3551. DOI: 10.3390/rs13183551

Kashani, A. G., M.J. Olsen, C.E. Parrish, and N. Wilson (2015). A review of LiDAR radiometric processing: From ad hoc intensity correction to rigorous radiometric calibration. *Sensors*, Vol. 15(11), pp. 28099-28128.

Kovanič, L., P. Blišťan, V. Zelizňakova, J. Palkova, J., and Baulovič (2019). Deformation investigation of the shell of rotary kiln using terrestrial laser scanning (TLS) measurement. *Metallurgija*, Vol. 58(3-4), pp. 311-314.

Li, X., Y. Li, X. Xie, and L. Xu (2018). Terrestrial laser scanner autonomous self-calibration with no prior knowledge of point-clouds. *IEEE Sensors Journal*, Vol. 18(22), pp. 9277-9285.

Li, D., J. Liu, L. Feng, Y. Zhou, P. Liu, and Y.F. Chen (2020). Terrestrial laser scanning assisted flatness quality assessment for two different types of concrete surfaces. *Measurement*, Vol. 154, pp. 107436.

Liu, M., X. Sun, Y. Wang, Y. Shao, and Y. You (2020). Deformation Measurement of Highway Bridge Head Based on Mobile TLS Data. *IEEE Access*, Vol. 8, pp. 85605-85615.

Marjasiewicz, M., and T. Malej (2014). Półautomatyczne modelowanie brył budynków na podstawie danych z lotniczego skaningu laserowego. *Archiwum Fotogrametrii, Kartografii i Teledetekcji*, Vol. 26.

Medić, T., Kuhlmann, H., and C. Holst (2020) Designing and Evaluating a User-Oriented Calibration Field for the Target-Based Self-Calibration of Panoramic Terrestrial Laser Scanners. *Remote Sens.*, *12*, 15. DOI: 10.3390/rs12010015

Muszyński, Z., and M. Wyjadłowski (2020). Assessment of surface parameters of VDW foundation piles using geodetic measurement techniques. *Open Geosciences*, Vol. 12(1), pp. 547-567.

Pinpin, L., Q. Wenge, C. Yunjian, and L. Feng (2021). Application of 3D laser scanning in underground station cavity clusters. *Advances in Civil Engineering*.

Reshetyuk, Y. (2006). Investigation and calibration of pulsed time-of-flight terrestrial laser scanners (*Doctoral dissertation, KTH)*.

Schnabel R., R. Wahl, and R. Klein (2007) Efficient RANSAC for Point-Cloud Shape Detection, *Computer graphics forum*.

Qian, X., and C. Ye (2014). NCC-RANSAC: a fast plane extraction method for 3-D range data segmentation. *IEEE transactions on cybernetics*, Vol. 44(12), pp. 2771-2783.

Wang, J., H. Kutterer, and X. Fang (2016). External error modelling with combined model in terrestrial laser scanning. *Survey review*, Vol. 48(346), pp. 40-50.

Wyczałek, I., A, Plichta, and M. Wyczałek (2017). Badania możliwości technicznych pomiaru płaskości powierzchni kinematyczną metodą trygonometryczną. *Zeszyty Naukowe. Inżynieria Środowiska/Uniwersytet Zielonogórski.*

Xiang, L., Y. Ding, Z. Wei, H. Zhang, and Z. Li (2021). Research on the Detection Method of Tunnel Surface Flatness Based on Point Cloud Data. *Symmetry*, Vol. 13(12), pp. 2239.

Xu, X., H. Yang, and B. Kargoll (2019). Robust and automatic modeling of tunnel structures based on terrestrial laser scanning measurement. *International Journal of Distributed Sensor Networks*, Vol. 15(11), pp. 1550147719884886.

Yang, H., and X. Xu (2021). Structure monitoring and deformation analysis of tunnel structure. *Composite Structures*, Vol. 276, pp. 114565.

Ye, C., S. Acikgoz, S. Pendrigh, E. Riley, and M.J. DeJong (2018). Mapping deformations and inferring movements of masonry arch bridges using point cloud data. *Engineering Structures*, Vol. 173, pp. 530-545.